

# Hydroxysafflor yellow A induces autophagy in human liver cancer cells by regulating Beclin 1 and ERK expression

ZIWEI CHEN<sup>1\*</sup>, LI LIU<sup>2\*</sup>, YUEYUN LIU<sup>1</sup>, SHUYAN WANG<sup>1</sup>, SHUJING ZHANG<sup>1</sup>, RUIJUAN DONG<sup>1</sup>,  
MINGYANG XU<sup>1</sup>, YICONG MA<sup>1</sup>, JINGJING WANG<sup>3</sup>, QIAN ZHANG<sup>1</sup> and PENG WEI<sup>1</sup>

<sup>1</sup>School of Traditional Chinese Medicine, Beijing University of Chinese Medicine, Beijing 100029;

<sup>2</sup>Institute of Chinese Materia Medica, China Academy of Chinese Medical Sciences, Beijing 100700;

<sup>3</sup>Oncology Microstart Intervention Department, Anyang Hospital of Traditional Chinese Medicine, Anyang, Henan 455001, P.R. China

Received July 4, 2019; Accepted January 30, 2020

DOI: 10.3892/etm.2020.8552

**Abstract.** Hydroxysafflor yellow A (HSYA) is a water-soluble component of the safflower (*Carthamus tinctorius*), and research has revealed that HSYA exhibits antitumor effects. In the present study, the effects of HSYA on the autophagy of a Hep-G2 liver cancer cell line, as well as the underlying mechanisms, were investigated. Hep-G2 cells were treated with HSYA and the viability of cells was measured using an MTT assay. Western blotting and immunofluorescence assays were performed to determine the expression of light chain 3 II (LC3-II) and p62, as well as the autophagy regulators Beclin 1 and ERK1/2. Transmission electron microscopy was performed to observe the formation of autophagosomes. The combined effects of HSYA and the autophagy inhibitor chloroquine (CQ) were also determined. The results revealed that the viability of Hep-G2 cells decreased with increasing concentrations of HSYA. Furthermore, LC3-II expression increased significantly and the level of p62 decreased significantly in the HSYA group compared with the control group. Additionally, an increase in Beclin 1 expression and a decrease in phosphorylated-ERK1/2 expression was observed in Hep-G2 cells treated with HSYA. Following treatment with CQ and HSYA, a significant increase in the viability of Hep-G2 cells was observed compared with the HSYA group. Collectively, the results indicated that HSYA induced autophagy by promoting the expression of Beclin 1 and inhibiting the phosphorylation

of ERK in liver cancer cells. Therefore, HSYA may serve as a potential therapeutic agent for liver cancer.

## Introduction

Liver cancer is one of the most common malignancies and is the second leading cause of morbidity and mortality worldwide. Furthermore, the incidence of liver cancer has increased in recent years (1). Surgery, as well as chemotherapy, radiation, targeted therapy and immunotherapy are currently the most common treatment strategies for liver cancer. However, these therapeutic methods, used either alone or in combination, have numerous limitations (2). Therefore, a number of previous studies have attempted to identify novel therapeutic agents for liver cancer derived from Traditional Chinese Medicine (TCM) (3,4). In China, it has been claimed that TCM has therapeutic advantages, including suppressing liver cancer progression, reducing surgical complications and increasing the sensitivity of cells to chemotherapy and radiotherapy (4,5). Furthermore, previous studies have reported that specific TCMs improve the function of the immune system in certain organisms and limit the detrimental effects of surgery, chemotherapy and radiotherapy (2,5). Therefore, TCM has gradually become a major focus for anti-tumor drug research and development.

Hydroxysafflor yellow A (HSYA) is a water-soluble component of the safflower (*Carthamus tinctorius*), which has been reported to exert pharmacological effects (6). Due to its potency and minimal side effects, the clinical use of HSYA has continued to increase since 2000 (7). Previous studies have reported that safflower exerts antitumor effects (8), and it has been reported that HSYA prevented pulmonary metastasis in liver cancer cells (9), induced apoptosis in human gastric carcinoma cells (BGC-823 cells) (10) and inhibited the growth of transplanted BGC-823 tumors. Another study also reported that the effect of HSYA on tumor capillary angiogenesis may be one of the mechanisms underlying its antineoplastic effect (11). However, to the best of our knowledge, the effects of HSYA on autophagy regulation in liver cancer cells have not yet been established.

Autophagy allows cells to survive under conditions of stress, including nutritional deficiency and injury, and

---

**Correspondence to:** Professor Qian Zhang or Dr Peng Wei, School of Traditional Chinese Medicine, Beijing University of Chinese Medicine, 11 North Third Ring Road East, Beijing 100029, P.R. China  
E-mail: zhang7017@163.com  
E-mail: weipeng@bucm.edu.cn

\*Contributed equally

**Key words:** hydroxysafflor yellow A, autophagy, light chain 3, Beclin 1, electron microscopy

also serves a critical role in maintaining cellular energy production (12). Autophagy has a two-way effect on tumor progression. A number of studies have reported that autophagy can inhibit tumorigenesis (13-15); however, when tumors form under oxygen-deficient conditions, autophagy is able to promote tumor growth and survival (16). Additionally, >30 autophagy-associated proteins have been identified, including light chain 3 (LC3), which was the first autophagosome protein marker to be discovered, the Beclin 1 complex and p62 (17-19). The expression of the Beclin 1 complex is closely associated with the occurrence and development of various tumors (18) and p62 is an autophagic substrate protein (19). Therefore, the three aforementioned proteins were selected as target proteins in the present study. Additionally, transmission electron microscopy was performed to detect the formation of autophagosomes. The results of the present study presented a theoretical and experimental basis for the development of novel antitumor drugs.

## Materials and methods

**Cell source.** The Hep-G2 cell line was provided by the Internal Medicine Laboratory of Dongzhimen Hospital and identified by Beijing Microread Genetics Co., Ltd. Cells were maintained in RPMI-1640 medium (HyClone; GE Healthcare Life Sciences) supplemented with 10% fetal bovine serum (Zhejiang Tianhang Biotechnology Co., Ltd.) and 1% penicillin-streptomycin. Cells were cultured at 37°C with 5% CO<sub>2</sub>.

**HSYA preparation.** A working solution of HSYA (C<sub>27</sub>H<sub>32</sub>O<sub>16</sub>; 32 µM/ml; National Institutes for Food and Drug Control) was prepared by dissolving 20 mg HSYA standard stock in 1.02 ml PBS. The solution was then sterilized using a 0.22-µm filter and stored at -20°C.

**MTT assay.** At 80-90% confluency, Hep-G2 cells were harvested and seeded (3x10<sup>4</sup> cells/ml) into a 96-well plate. The cells were incubated at 37°C with 5% CO<sub>2</sub> for 24 h. HSYA was added to the cells to a final concentration of 0.5, 1, 2, 4, 8 or 16 µM; the concentrations were selected based on a preliminary study, as well as IC<sub>50</sub> values obtained from the literature (64.0±4.6 µM) (20). At 24 h post-transfection, 10 µl MTT solution was added to each well and the plate was incubated for a further 4 h at 37°C. Subsequently, 100 µl DMSO (Sigma-Aldrich; Merck KGaA) was added to each well and the plate was incubated for 10 min with shaking at room temperature. Absorbance was measured at a wavelength of 570 nm (reference wavelength, 630 nm) using a multi-functional full-wavelength microplate reader and the optimal inhibitory concentration was recorded. 50 mM chloroquine (CQ) solution was prepared by dissolving 0.016 g CQ (cat. no. KH-0005; Key Organics) in 100 µl DMSO and 900 µl RPMI-1640 medium (supplemented with 10% FBS and 1% penicillin streptomycin). The solution was then sterilized using a 0.22-µm filter and stored at 4°C and diluted to 10 µM as previously described (21-24).

**Observation of cell morphology.** Hep-G2 cells (3x10<sup>4</sup> cells/ml) were seeded into 6-well plates and incubated for 24 h at 37°C. Subsequently, the RPMI-1640 medium was discarded, 2 µM

HSYA was added and the plates were incubated for 24 h at 37°C. Cells were photographed in three randomly selected fields under an inverted microscope (CKX41; Olympus Corporation) at x400 magnification.

**Transmission electron microscopy.** Hep-G2 cells (3x10<sup>4</sup> cells/ml) were plated in six-well plates and incubated for 24 h at 37°C. Subsequently, 2 µM HSYA was added and the cells were incubated for a further 6 h at 37°C. Cells were harvested, fixed with 2.5% glutaraldehyde for 12 h at 4°C and washed with PBS three times for 5 min each time. The cells were further treated with 1% osmium tetroxide for 3 h at room temperature. Subsequently, cell samples were dehydrated using an ascending ethanol and acetone series, and embedded using 1.5% DMP-30 and epoxy resin, gradient polymerization was performed on the cell samples using the following conditions: 35°C for 12 h, 45°C for 12 h and 60°C for 24 h. Subsequently, the samples were sliced into 70-nm thick sections using a microtome prior to staining with uranyl acetate and lead citrate for 2 h at room temperature. The samples were observed using a Tecnai™ Spirit transmission electron microscope (magnification, x18,500 and x30,000).

**Immunofluorescence detection.** Hep-G2 cells were treated with 2 µM HSYA and incubated for 6 h at 37°C. Subsequently, the cells were harvested, fixed in 4% paraformaldehyde for 15 min at room temperature, and washed in 0.1% Triton X-100 at room temperature prior to blocking [5% FBS; 1% FGS (cat. no. SL038; Beijing Solarbio Science & Technology Co., Ltd. and 0.3% Triton X-100 (cat. no. P0096; Beyotime Institute of Biotechnology)] at room temperature for 1 h. Cells were incubated with an anti-LC3A/B primary antibody (cat. no. 4108; 1:50; Cell Signaling Technology, Inc.) at 4°C overnight, followed by a second incubation step with a goat anti-rabbit secondary antibody (cat. no. A-1108; 1:200; Thermo Fisher Scientific, Inc.) IgG (H+L) at room temperature for 2 h. Subsequently, the samples were sealed with a water-soluble mounting media containing DAPI and three fields of view were observed under an inverted fluorescence microscope (magnification, x400; Olympus Corporation).

**Western blotting.** Total protein was extracted from Hep-G2 cells using RIPA buffer (Applygen Technology Co., Ltd.) supplemented with 2% protease inhibitor and 1% protein phosphatase inhibitor according to the manufacturer's instructions. Total protein was quantified using a bicinchoninic acid assay and 20 µg of protein/lane were separated via SDS-PAGE (7, 10 or 13% due to the different molecular weights of the samples). Subsequently, separated proteins were transferred to PVDF membranes and blocked with 5% non-fat milk at room temperature for 1 h. The membranes were incubated at 4°C overnight with primary antibodies targeted against the following: LC3A/B (1:500), Beclin 1 (cat. no. 11306; 1:5,000; ProteinTech Group, Inc.), p62 (cat. no. 18420; 1:2,000; ProteinTech Group, Inc.), ERK1/2 (cat. no. AF0155; 1:2,500; Affinity Biosciences), phosphorylated (p)-ERK1/2 (cat. no. AF1015; 1:1,500; Affinity Biosciences), GAPDH (cat. no. HRP-6004; 1:50,000; ProteinTech Group, Inc.) and β-actin (cat. no. HRP-6008; 1:20,000; ProteinTech Group,

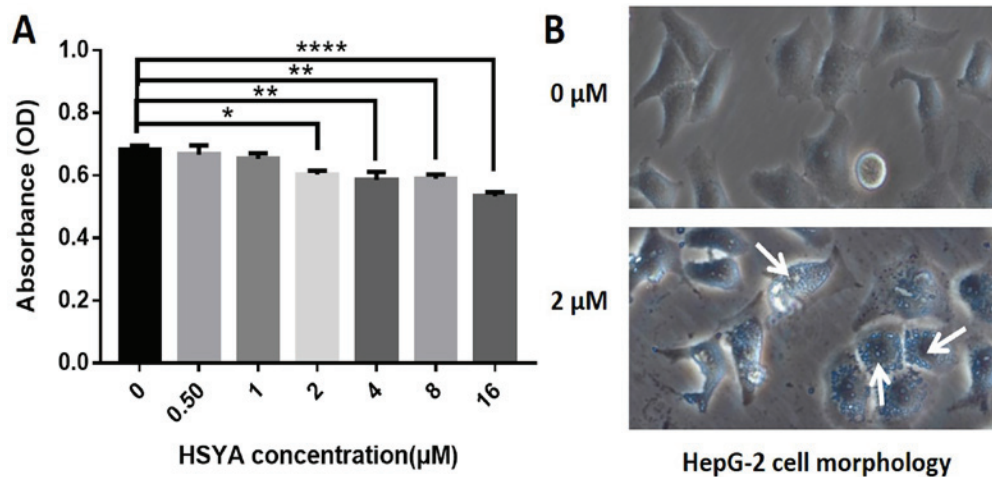


Figure 1. HSYA inhibits the viability of Hep-G2 cells. (A) MTT assay demonstrated that treatment of Hep-G2 cells with different concentrations of HSYA significantly increased cell viability in the 2 to 16  $\mu$ M HSYA groups compared with the 0  $\mu$ M HSYA group, the effects of which were dose dependent. (B) Microscopically, a large number of vacuoles (as indicated by the arrows) were observed in Hep-G2 cells treated with 2  $\mu$ M HSYA for 24 h, compared with the control group (magnification, x400). \* $P$ <0.05, \*\* $P$ <0.01 and \*\*\*\* $P$ <0.001 vs. the 0  $\mu$ M HSYA group. HSYA, hydroxysafflower yellow A.

Inc.). After washing with TBS-Tween, the membranes were incubated with a goat anti-mouse (cat. no. ZB-2305; 1:20,000; Zhongshan Golden Bridge Bio-Technology) immunoglobulin G (IgG) (H+L) or goat anti-rabbit (cat. no. CW0103S; 1:5,000; Kangwei Century) IgG (H+L) secondary antibody for 1 h at room temperature. Protein bands were visualized using the horseradish peroxidase-conjugated ECL Luminol substrate (Applygen Technologies, Inc.). Protein expression was quantified using AlphaView software (version 3.4; Alpha Innotech gel imager) with GAPDH or  $\beta$ -actin as the loading control. Western blot experiments for each protein were repeated at least three times.

**Statistical analysis.** Data are presented as the mean  $\pm$  standard deviation. Statistical differences were calculated using the Student's t-test, one-way ANOVA followed by Dunnett's post hoc test or two-way ANOVA followed by Sidak's multiple comparison test. Statistical analyses were performed using SPSS software (version 20.0; IBM Corp.).  $P$ <0.05 was considered to indicate a statistically significant difference.

## Results

**HSYA reduces the viability of Hep-G2 cells.** Hep-G2 cells were treated with six different concentrations of HSYA and cell viability was assessed using an MTT assay. The results revealed that cell viability was decreased following HSYA treatment compared with the control group, in a dose dependent manner (Fig. 1A). The 2-16  $\mu$ M HSYA groups exhibited a significant decrease in cell viability compared with the control group (Fig. 1A). Therefore, 2  $\mu$ M HSYA was selected for subsequent experimentation based on the minimum effective dose.

Hep-G2 cells in the control group were morphologically confirmed to be in good condition, displaying fullness, clear cell boundaries and close adherence (Fig. 1B). After incubation for 24 h with 2  $\mu$ M HSYA, Hep-G2 cells exhibited a large number of vacuoles and cellular debris, suggesting that autophagy had occurred (Fig. 1B).

**HSYA affects the expression of autophagy-associated proteins.** To identify autophagy, the autophagy marker protein, LC3 and its substrate protein, p62, were detected using western blotting. The results revealed that the LC3-II content increased in a time-dependent manner in the HSYA cells, peaking at the 6-h time point to a level significantly higher compared with the control group. Furthermore, LC3-II content decreased between 6 and 24 h in HSYA groups. By contrast, the protein expression of p62 was significantly reduced by 46% at 6 h, and there was no significant difference at 24 h compared with the control group (Fig. 2).

**HSYA induces autophagy in Hep-G2 cells.** Following the addition of 2  $\mu$ M HSYA for 6 h, the distribution of LC3 protein in Hep-G2 cells was observed by immunofluorescence staining. The nucleus exhibited blue coloration and LC3 protein expression was indicated in green (Fig. 3). The results suggested that the green fluorescence in the control group was diffusely distributed; however, a large number of green clusters were visible within the cells of the HSYA group, indicating an increase in LC3 protein expression. At 6 h, the increase in autophagy marker protein LC3 and decrease in autophagy substrate p62 expression further suggested that HSYA-induced autophagy had occurred (Fig. 2B and D).

To further investigate autophagy, the cell morphology assays were visualized under a transmission electron microscope. Due to the higher resolution of transmission electron microscopy compared with fluorescence microscopy, the microstructures of pre-autophagosomes, autophagosomes and autolysosomes that were present during autophagy formation were clear. When autophagy begins, the phagocytic vacuoles of the bowl-shaped bilayer membrane structure form and continuously extend into the cytoplasm, enclosing the organelles to form autophagosomes with a vesicular structure and the encapsulated organelles are subsequently degraded (25). In the present study, the early (AVi) and late (AVd) autophagosomes were broadly classified depending on whether the envelope structure in the

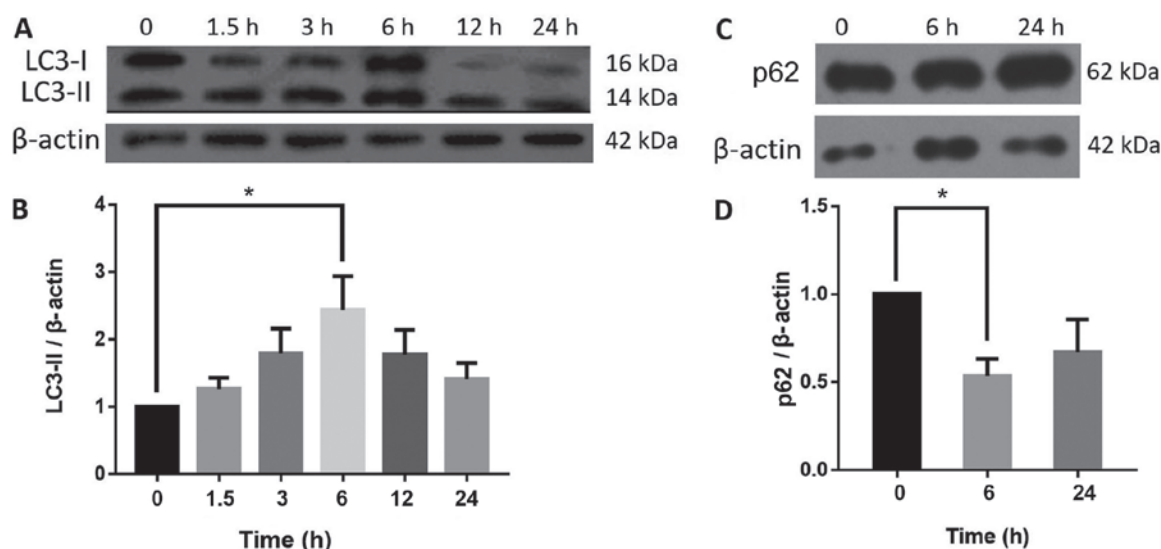


Figure 2. Effect of 2  $\mu$ M HSYA on LC3 and p62 protein expression. Protein levels of LC3-II were determined by (A) western blot analysis and (B) quantified. Protein levels of p62 were determined by (C) western blot analysis and (D) quantified. \* $P < 0.05$  vs. the control group. HSYA, hydroxysafflor yellow A; LC3, light chain 3.

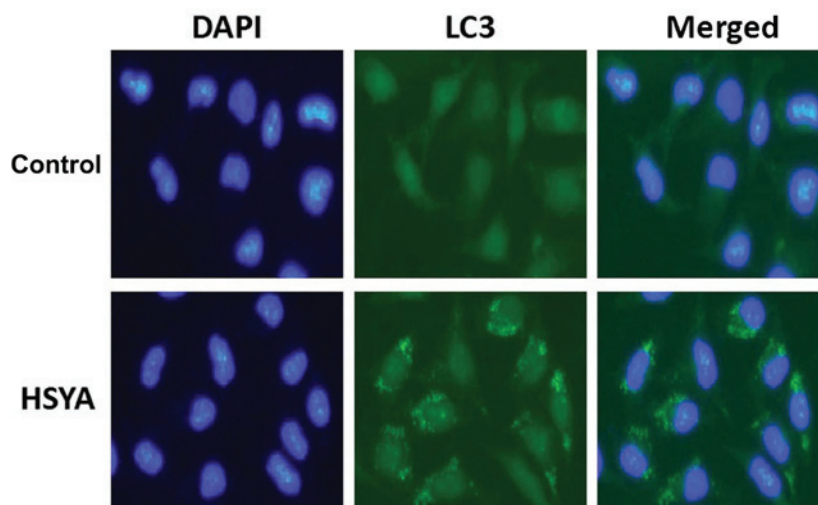


Figure 3. Effect of 2  $\mu$ M HSYA on the distribution of LC3 protein in Hep-G2 cells. The nucleus is indicated by blue and LC3 expression is indicated by green (magnification,  $\times 400$ ). HSYA, hydroxysafflor yellow A; LC3, light chain 3.

vesicles remained intact. The two structures distinguished the different stages of autophagy, to determine whether autophagy had occurred. After treatment with 2  $\mu$ M HSYA for 6 h, Hep-G2 cells were observed under a transmission electron microscope. Part of the bilayer membrane structure of AVi enveloped the contents prior to degradation (Fig. 4A). At the same time, autophagosomes were fused with lysosomes to form autolysosomes and the encapsulated contents were degraded to form a single-layer membrane structure, the AVd. The control group exhibited fewer autophagosomes compared with the HSYA group (Fig. 4A and B). Furthermore, AVi and AVd structures were increased in the HSYA group, indicating that autophagy had occurred (Fig. 4C and D). Following quantitative analysis, the degree of autophagy in the 6 h group, regardless of AVi or AVd status, was higher compared with the 0 h group. The AVi status of the 6 h group was significantly increased compared

with the 0 h group (Fig. 5). Collectively, the results suggested that 2  $\mu$ M HSYA induced autophagy in Hep-G2 cells, most significantly at the 6 h time point.

**HSYA and CQ increase the viability of Hep-G2 cells.** After observing HSYA-induced autophagy, the effects of the 10  $\mu$ M autophagy inhibitor CQ on the viability of Hep-G2 cells were assessed. CQ was combined with HSYA and alterations in hepatoma cell viability were determined using an MTT assay. The results revealed that HSYA (2  $\mu$ M for 6 h) treatment reduced hepatoma cell viability, with a significant decrease of 13% compared with the control group (Fig. 6A). However, the combination of CQ and HSYA increased cell viability at 18 and 24 h, compared with the use of either reagent alone (Fig. 6B and C). At 18 h, the viability of the combination group was significantly increased by 58% compared with the HSYA group (Fig. 6C).



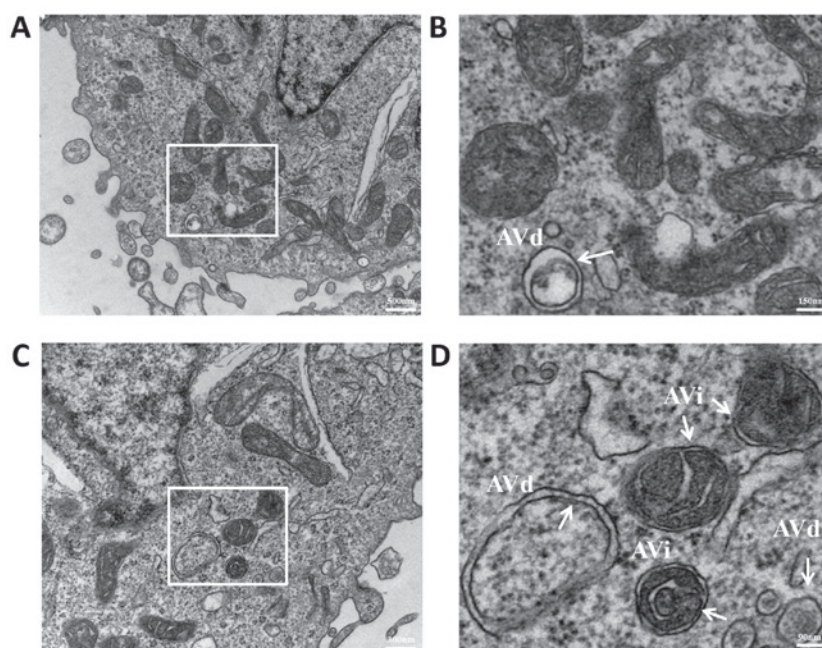


Figure 4. Effect of HSYA on autophagy microstructure. (A) TEM image and (B) magnified image of autophagosome structures in the control group. (C) TEM image and (D) magnified image of autophagosome structures in the 2  $\mu$ M HSYA group. The white arrow indicates the cell bilayer membrane structure of the autophagosome. The white boxes indicate the enlarged areas. HSYA, hydroxysafflor yellow A; TEM, transmission electron microscope; AVi, early autophagosome; AVd, late autophagosome.

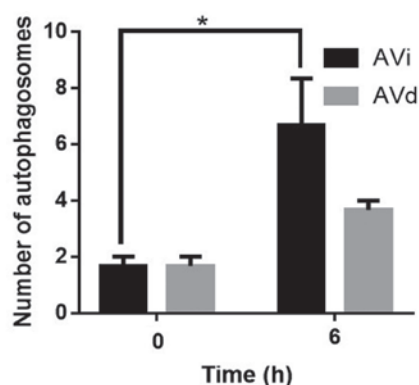


Figure 5. Quantification of the number of autophagosomes. Number of autophagosomes in control (0 h) and 2  $\mu$ M HSYA groups (6 h). \* $P$ <0.05 vs. the control group. HSYA, hydroxysafflor yellow A; AVi, early autophagosome; AVd, late autophagosome.

*HSYA affects autophagy by regulating the expression of Beclin 1 and ERK.* To determine the possible mechanisms of autophagy regulation, western blot analysis was performed to detect the expression of the autophagy regulator proteins Beclin 1 and ERK in Hep-G2 cells. Beclin 1 is an important protein involved in the regulation of autophagy and the activation of ERK1/2 can be detected in numerous autophagic processes (26,27). The protein expression of Beclin 1 increased significantly by 44% in Hep-G2 cells following the addition of 2  $\mu$ M HSYA for 6 h. The levels of Beclin 1 protein expression increased slightly at 24 h compared with the control group (Fig. 7A and B). Additionally, the ratio of p-ERK1/2 to total ERK1/2 decreased significantly by 31% in the HSYA group at 6 h compared with the control group (Fig. 8A and B). The results indicated that HSYA influenced

autophagy by regulating Beclin 1 and ERK protein expression.

## Discussion

Liver cancer is the second most common cause of cancer-associated death worldwide, and the incidence and mortality rates have steadily increased (28). At present, surgery and western pharmaceutical drugs are the two primary strategies for treating tumors. However, unwanted side effects and drug resistance have led to increased research into novel multi-faceted and multi-targeting antitumor drugs, including a focus on TCM (4,5).

TCM adjuvant treatments may have significant advantages in improving the quality of life and prolonging the survival time of patients with liver cancer compared with standard treatment strategies (2). HSYA is one of the primary water-soluble, active ingredients of the TCM safflower. HSYA has been reported to promote apoptosis in abnormal human umbilical vein endothelial cells (29) and to suppress the inflammatory responses of BV2 microglial cells after oxygen-glucose deprivation (30). In the present study, an MTT assay revealed that HSYA reduced the viability of liver cancer cells and a large number of vacuoles and a small amount of cell debris were microscopically observed in HSYA-treated cells, suggesting that HSYA induced autophagy. A previous study had determined that the  $IC_{50}$  value for HSYA was  $64.0 \pm 4.6 \mu$ M (20); therefore, a final concentration of 2  $\mu$ M HSYA was used in the present study, and the effects on cellular viability were considered to be the result of the pharmacological properties, rather than toxic side effects.

Autophagy is referred to as cellular self-digestion. The autophagic membrane envelops areas of the cytoplasm to form

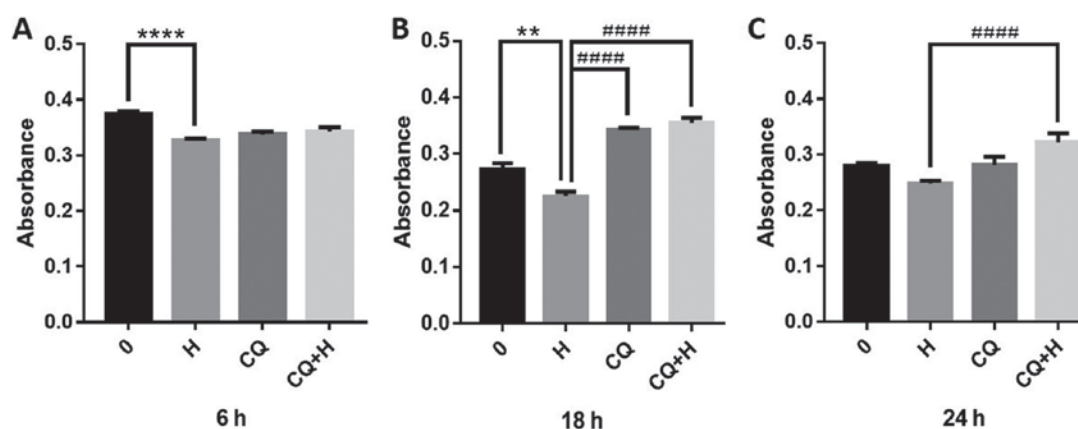


Figure 6. Combined treatment with 2  $\mu$ M HSYA and CQ enhances the viability of Hep-G2 cells. A significant difference was identified between the control group and the HSYA group at (A) 6 h, (B) 18 h and (C) 24 h. \*\* $P < 0.01$  and \*\*\*\* $P < 0.0001$  vs. the control group; ##### $P < 0.0001$  vs. the HSYA group. HSYA, hydroxysafflor yellow A; CQ, chloroquine; H, HSYA.

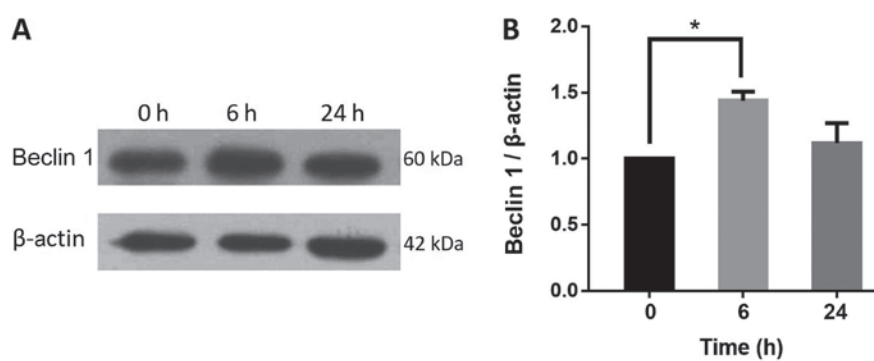


Figure 7. HSYA increases the expression of Beclin 1. Protein levels were determined by (A) western blot analysis. (B) Quantification of western blotting results. Western blot analysis results suggested that Beclin1 protein expression was most significantly increased after 6 h treatment with HSYA compared with the control group. \* $P < 0.05$  vs. the control group. HSYA, hydroxysafflor yellow A.

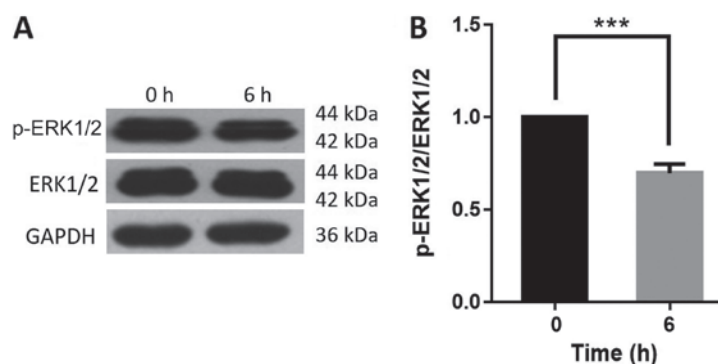


Figure 8. HSYA reduces the ratio of p-ERK1/2 to total ERK1/2 in Hep-G2 cells. Protein levels were determined by (A) western blot analysis. (B) Quantification of western blotting results. \*\*\* $P < 0.001$  vs. the control group. HSYA, hydroxysafflor yellow A; p, phosphorylated.

an autophagosome, encompassing organelles and proteins for degradation (25). The autophagosome then fuses with a lysosome to form an autolysosome, which subsequently degrades the encapsulated contents, the products of degradation provide raw materials and are a means of recycling existing cellular material (25). AVi structures contain morphologically intact cytoplasm, which is comparable to the surrounding cytoplasm (25). By contrast, AVd structures contain material that can still be recognized as cytoplasmic. However, the

ribosomes are partially degraded, resulting in a more electron dense cytoplasm compared with the surroundings. Only vacuoles containing cytoplasmic material can be considered autophagic (25). In addition, an autophagy landmark LC3 protein test is required to determine whether autophagy has occurred (17).

LC3 was the first autophagosome marker protein to be identified in LC3 synthesis (17) and exists in a soluble form (LC3-I) in the cytosol. When autophagy occurs, LC3-I is

converted to LC3-II with the help of autophagy complexes. LC3-II is an autophagosome marker with membrane-binding ability, which is also localized to autophagic membranes and its expression is related to the number of autophagosomes (31). Theoretically, increases in the LC3-II/LC3-I ratio indicate the occurrence of autophagy (32). However, LC3-II and LC3-I have different sensitivity to antibodies thus the LC3-II/LC3-I ratio was different than expected. Therefore, to determine the degree of autophagic viability, it is necessary to observe the entire process, including the degradation of the autophagy substrate p62 (32).

In the present study, treatment of Hep-G2 cells with 2  $\mu$ M HSYA for 6 h increased the LC3-II content and decreased the p62 content. In the HSYA group, immunofluorescence detection suggested that the LC3 protein aggregated within the cells at 6 h and electron microscopy revealed that AVi and AVd structures were present, confirming that autophagy had occurred. In summary, the results demonstrated that HSYA induced autophagy in Hep-G2 cells and that autophagy occurred at the highest rate at the 6 h time point.

He *et al* (33) reported that the use of a chalcone derivative, Chal-24, induced autophagy and promoted cancer cell apoptosis, indicating that autophagic induction may serve as a novel treatment strategy for tumors. In the present study, 2  $\mu$ M HSYA significantly reduced cell viability and CQ, a common autophagy inhibitor, increased cell viability. CQ + HSYA treatment also increased liver cancer cell viability compared with control cells. The results suggested that CQ inhibited HSYA-induced autophagy and increased cell viability. Furthermore, it could be suggested that HSYA reduced the viability of cells by inducing autophagy, further suggesting that autophagy inducers may serve as a potential treatment strategy to enhance the effects of HSYA in liver cancer.

Beclin 1 is an important protein involved in the regulation of autophagy (34), which promotes autophagy by localizing to autophagic precursors (35). In the present study, the addition of 2  $\mu$ M HSYA to Hep-G2 cells significantly increased Beclin 1 protein expression levels at the 6 h time point, indicating that autophagy was induced by regulating Beclin 1 in liver cancer cells.

ERK1/2 activation can be detected in various autophagic processes and can influence the proliferation of tumor cells via autophagy (26,27). p-ERK1/2 proteins directly phosphorylate the S664 residue of the tuberlin protein, thereby inhibiting autophagy (36). Furthermore, upregulating the p-ERK/ERK ratio can inhibit autophagy in the hippocampus of mice (37). Therefore, it was hypothesized that p-ERK/ERK was associated with autophagy. In the present study, HSYA significantly decreased the p-ERK/ERK content of Hep-G2 cells. The results indicated that HSYA significantly inhibited the phosphorylation of ERK1/2 and subsequently induced autophagy and inhibited the viability of liver cancer cells.

During the process of autophagosome-to-autolysosome formation, the Beclin 1 complex and ERK1/2 serve an important role in regulating autophagy (38). The results of the present study indicated an increase in LC3-II and a decrease in p62 content following HSYA treatment of Hep-G2 cells, suggesting an induction of autophagy. Therefore, the present study suggested that the Beclin 1 complex may promote the

occurrence of autophagy; a process that may be indirectly inhibited by ERK1/2.

In combination with previous research, the results of the present study indicated that HSYA had various effects on liver and gastric cancer cells, including preventing metastasis, inducing apoptosis and reducing viability (10). The results of the current study also suggested that HSYA induced autophagy by increasing the expression of Beclin 1 and inhibiting the phosphorylation of ERK in human liver cancer cells, therefore indicating that HSYA exhibited antitumor viability. To conclude, HSYA may serve as a potential therapeutic for liver cancer by enhancing autophagy.

## Acknowledgements

Not applicable.

## Funding

The present study was supported by The National Natural Science Foundation of China (grant nos. 31500640, 30572436 and 31800652).

## Availability of data and materials

The datasets used and/or analyzed during the current study are available from the corresponding author on reasonable request.

## Authors' contributions

QZ and PW conceived and designed the study. ZC, LL and YM performed the experiments. YL, SZ and JW analyzed the data. SW, RD and MX provided reagents and performed immunofluorescence and microscopy experiments. ZC and LL wrote the manuscript. All authors read and approved the final manuscript.

## Ethics approval and consent to participate

Not applicable.

## Patient consent for publication

Not applicable.

## Competing interests

The authors declare that they have no competing interests.

## References

1. Bray F, Ferlay J, Soerjomataram I, Siegel RL, Torre LA and Jemal A: Global cancer statistics 2018: GLOBOCAN estimates of incidence and mortality worldwide for 36 cancers in 185 countries. *CA Cancer J Clin* 68: 394-424, 2018.
2. Qi F, Zhao L, Zhou A, Zhang B, Li A, Wang Z and Han J: The advantages of using traditional Chinese medicine as an adjunctive therapy in the whole course of cancer treatment instead of only terminal stage of cancer. *Biosci Trends* 9: 16-34, 2015.
3. Gao X, Wang Y, Li Y, Wang Y, Yan M, Sun H, Chen S and Pan X: Huguangpian, a traditional Chinese medicine, inhibits liver cancer growth in vitro and in vivo by inducing autophagy and cell cycle arrest. *Biomed Pharmacother* 120: 109469, 2019.



4. Liao X, Bu Y and Jia QA: Traditional Chinese medicine as supportive care for the management of liver cancer: Past, present, and future. *Genes Dis* 2019. doi.org/10.1016/j.gendis.2019.10.016.
5. Xie G, Cui Z, Peng K, Zhou X, Xia Q and Xu D: Aidi injection, a traditional Chinese medicine injection, could be used as an adjuvant drug to improve quality of life of cancer patients receiving chemotherapy: A propensity score matching analysis. *Integr Cancer Ther* 18: 1534735418810799, 2019.
6. Jin M, Xue CJ, Wang Y, Dong F, Peng YY, Zhang YD, Zang BX and Tan L: Protective effect of hydroxysafflor yellow A on inflammatory injury in chronic obstructive pulmonary disease rats. *Chin J Integr Med* 25: 750-756, 2019.
7. Fan L, Pu R, Zhao HY, Liu X, Ma C, Wang BR and Guo DA: Stability and degradation of hydroxysafflor yellow A and anhydrosafflor yellow B in the safflower injection studied by HPLC-DAD-ESI-MSn. *J Chin Pharm Sci* 20: 47-56, 2011.
8. Ao H, Feng W and Peng C: Hydroxysafflor yellow A: A promising therapeutic agent for a broad spectrum of diseases. *Evid Based Complement Alternat Med* 2018: 8259280, 2018.
9. Ma L, Liu L, Ma Y, Xie H, Yu X, Wang X, Fan A, Ge D, Xu Y, Zhang Q and Song C: The role of E-cadherin/ $\beta$ -catenin in hydroxysafflor yellow A inhibiting adhesion, invasion, migration and lung metastasis of hepatoma cells. *Biol Pharm Bull* 40: 1706-1715, 2017.
10. Liu L, Si N, Ma Y, Ge D, Yu X, Fan A, Wang X, Hu J, Wei P, Ma L, *et al*: Hydroxysafflor-yellow A induces human gastric carcinoma BGC-823 cell apoptosis by activating peroxisome proliferator-activated receptor gamma (PPAR $\gamma$ ). *Med Sci Monit* 24: 803-811, 2018.
11. Xi SY, Zhang Q, Liu CY, Xie H, Yue LF and Gao XM: Effects of hydroxy safflower yellow-A on tumor capillary angiogenesis in transplanted human gastric adenocarcinoma BGC-823 tumors in nude mice. *J Tradit Chin Med* 32: 243-248, 2012.
12. Levine B and Klionsky DJ: Development by self-digestion: Molecular mechanisms and biological functions of autophagy. *Dev Cell* 6: 463-477, 2004.
13. Liu W, Zeng X, Yin Y, Li C, Yang W, Wan W, Shi L, Wang G, Tao K and Zhang P: Targeting the WEE1 kinase strengthens the antitumor activity of imatinib via promoting KIT autophagic degradation in gastrointestinal stromal tumors. *Gastric Cancer* 23: 39-51, 2020.
14. Dent P, Booth L and Poklepovic A: Metabolism of histone deacetylase proteins opsonizes tumor cells to checkpoint inhibitory immunotherapies. *Immunometabolism* 2: e200002, 2020.
15. Deng X, Guan W, Qing X, Yang W, Que Y, Tan L, Liang H, Zhang Z, Wang B, Liu X, *et al*: Ultrafast low-temperature photo-thermal therapy activates autophagy and recovers immunity for efficient antitumor treatment. *ACS Appl Mater Interfaces* 12: 4265-4275, 2020.
16. Rautou PE, Mansouri A, Lebrech D, Durand F, Valla D and Moreau R: Autophagy in liver diseases. *J Hepatol* 53: 1123-1134, 2010.
17. Tanida I, Ueno T and Kominami E: LC3 conjugation system in mammalian autophagy. *Int J Biochem Cell Biol* 36: 2503-2518, 2004.
18. Liu J, Lin Y, Yang H, Deng Q, Chen G and He J: The expression of p33(ING1), p53, and autophagy-related gene Beclin1 in patients with non-small cell lung cancer. *Tumour Biol* 32: 1113-1121, 2011.
19. Masuda S, Mizukami S, Eguchi A, Ichikawa R, Nakamura M, Nakamura K, Okada R, Tanaka T, Shibutani M and Yoshida T: Immunohistochemical expression of autophagosome markers LC3 and p62 in preneoplastic liver foci in high fat diet-fed rats. *J Toxicol Sci* 44: 565-574, 2019.
20. Song H, Wang D, Li J, Yang Y, Mu X and Bai X: Hydroxysafflor yellow A inhibits proliferation and migration of human hepatocellular carcinoma cells and promotes apoptosis via PI3K pathway. *Tumor* 38: 830-839, 2018.
21. Zhang C, Jia XJ, Wang K, Bao JL, Li P, Chen MW, Wan JB, Su HX, Mei ZN and He CW: Polyphyllin VII induces an autophagic cell death by activation of the JNK pathway and inhibition of PI3K/AKT/mTOR pathway in hepG2 cells. *PLoS One* 11: e0147405, 2016.
22. Li T, Tang ZH, Xu WS, Wu GS, Wang YF, Chang LL, Zhu H, Chen XP, Wang YT, Chen Y and Lu JJ: Platycodin D triggers autophagy through activation of extracellular signal-regulated kinase in hepatocellular carcinoma HepG2 cells. *Eur J Pharmacol* 749: 81-88, 2015.
23. Li T, Wen L and Cheng B: Cordycepin alleviates hepatic lipid accumulation by inducing protective autophagy via PKA/mTOR pathway. *Biochem Biophys Res Commun* 516: 632-638, 2019.
24. Lu Y, Zhang R, Liu S, Zhao Y, Gao J and Zhu L: ZT-25, a new vacuolar H(+)-ATPase inhibitor, induces apoptosis and protective autophagy through ROS generation in HepG2 cells. *Eur J Pharmacol* 771: 130-138, 2016.
25. Eskelinen EL: Fine structure of the autophagosome. *Methods Mol Biol* 445: 11-28, 2008.
26. Wang M, Qiu S and Qin J: Baicalein induced apoptosis and autophagy of undifferentiated thyroid cancer cells by the ERK/PI3K/Akt pathway. *Am J Transl Res* 11: 3341-3352, 2019.
27. Li HH, Song XX, Liu B and Yang WP: UNBS5162 as a novel naphthalimide holds efficacy in human gastric carcinoma cell behaviors mediated by AKT/ERK signaling pathway. *Drug Dev Ind Pharm* 45: 1306-1312, 2019.
28. Sia D, Villanueva A, Friedman SL and Llovet JM: Liver cancer cell of origin, molecular class, and effects on patient prognosis. *Gastroenterology* 152: 745-761, 2017.
29. Si N, Wang J, Xu Y, Liu L, Wang X, Sun H, Lin Z, Wang X, Liu L, Zhang Q, *et al*: Inductive effect of hydroxyl safflower yellow-A on apoptosis in abnormal HUVEC via the mitochondrial pathway. *J Trad Chin Med Sci* 2: 25-31, 2015.
30. Li J, Zhang S, Lu M, Chen Z, Chen C, Han L, Zhang M and Xu Y: Hydroxysafflor yellow A suppresses inflammatory responses of BV2 microglia after oxygen-glucose deprivation. *Neurosci Lett* 535: 51-56, 2013.
31. Hale AN, Ledbetter DJ, Gawriluk TR and Rucker EB 3rd: Autophagy: Regulation and role in development. *Autophagy* 9: 951-972, 2013.
32. Yang Y, He P and Li N: The antitumor potential of extract of the oak bracket medicinal mushroom *Inonotus baumii* in SMMC-7721 tumor cells. *Evid Based Complement Alternat Med* 2019: 1242784, 2019.
33. He W, Wang Q, Srinivasan B, Xu J, Padilla MT, Li Z, Wang X, Liu Y, Gou X, Shen HM, *et al*: A JNK-mediated autophagy pathway that triggers c-IAP degradation and necroptosis for anticancer chemotherapy. *Oncogene* 33: 3004-3013, 2014.
34. Sutton MN, Huang GY, Liang X, Sharma R, Reger AS, Mao W, Pang L, Rask PJ, Lee K, Gray JP, *et al*: DIRAS3-Derived peptide inhibits autophagy in ovarian cancer cells by binding to Beclin1. *Cancers (Basel)* 11: E557, 2019.
35. Kang R, Zeh HJ, Lotze MT and Tang D: The Beclin 1 network regulates autophagy and apoptosis. *Cell Death Differ* 18: 571-580, 2011.
36. Ma L, Chen Z, Erdjument-Bromage H, Tempst P and Pandolfi PP: Phosphorylation and functional inactivation of TSC2 by Erk implications for tuberous sclerosis and cancer pathogenesis. *Cell* 121: 179-193, 2005.
37. Zhu J, Liao S, Zhou L and Wan L: Tanshinone IIA attenuates A $\beta$ <sub>25-35</sub>-induced spatial memory impairment via upregulating receptors for activated C kinase1 and inhibiting autophagy in hippocampus. *J Pharm Pharmacol* 69: 191-201, 2016.
38. Pan H, Wang Y, Na K, Wang Y, Wang L, Li Z, Guo C, Guo D and Wang X: Autophagic flux disruption contributes to *Ganoderma lucidum* polysaccharide-induced apoptosis in human colorectal cancer cells via MAPK/ERK activation. *Cell Death Dis* 10: 456, 2019.



This work is licensed under a Creative Commons Attribution-NonCommercial-NoDerivatives 4.0 International (CC BY-NC-ND 4.0) License.